The Application of a Geometric Optical Canopy Reflectance Model to Semiarid Shrub Vegetation

Janet Franklin and Debra L. Turner

Abstract—**The Li–Strahler [7] canopy model was tested, using SPOT HRV XS imagery, for semiarid shrub vegetation, based on 26 small (1-ha) sites in five classes of shrub vegetation, two dominated by tarbush (*Flourensia cernua*), one by creosote bush (*Larrea tridentata*), and two by mesquite (*Prosopis glandulosa*). The model was driven by reflectance values derived from June and September imagery. While predictions of crown size and density for individual sites had a large average error of 35%, the predictions of shrub size and density were reasonably accurate when grouped by shrub class. The aggregated predictions for a number of stands within a class were accurate to within one or two standard errors of the observed average value. Accuracy was highest but predictions were biased for some classes (size was underestimated) when the nonrandom shrub pattern was characterized for the class based on the average coefficient of determination of density. Results based on June data were not better than September because the hypothesized lower background "noise" (e.g., less green herbaceous cover that could be confused with shrub cover in the simple reflectance model) was not observed in the June data. This could have been due to the poor radiometric quality of the June image.**

Keywords—**Remote sensing, digital image, Li–Strahler canopy reflectance model, semiarid shrub vegetation.**

I. Introduction

Simple, invertible models of the multispectral response of partially vegetated land surfaces are needed in order to use satellite imagery for monitoring semiarid vegetation over large areas. Models of vegetation canopy reflectance based on radiative transfer theory (reviewed in [1]) may not be invertible using existing satellite imagery of natural, sparse vegetation. Spectral vegetation indices, while they have proven useful [2]–[4], do not go far enough toward isolating the vegetation signal from the background in semiarid vegetation with complex spatial and phenological patterns [5], [6]. In semiarid vegetation formations the vegetation component does not always dominate spatially averaged remotely sensed measurements.

A series of reflectance models, developed by A. H. Strahler and others, treats woody vegetation canopies as an assemblage of discrete three-dimensional objects, illuminated at an angle and casting shadows on a contrasting background [7]-[12]. By modeling a plant canopy as a collection of regular geometric shapes, optical principles and parallel-ray geometry can be used to predict the bidirectional reflectance of a shrubland, woodland, or forest [11]. Most relevant to the present study, these models have been developed for the purpose of inverting them using multispectral digital imagery. Vegetation parameters (plant size and density) can be estimated from remotely sensed reflectance measurements using the variance in the spectral response of a vegetation stand as seen in a digital image [7]. When the sensor field of view is one or two orders of magnitude larger than the average plant size, as is the case for the principal Earth resources satellites (Landsat and SPOT) and many vegetation formations, the pattern of plant, shadow, and background is a major source of spatial variance in the image [13], [14].

The objective of this study was to estimate average plant size and density from SPOT High Resolution Visible (HRV) multispectral (XS) imagery for test sites in Chihuahuan desert shrub communities using the Li–Strahler [7] model. Estimates of woody vegetation structure for large areas are needed in order to model primary production and biogeochemical cycling [15], and land surface–climate interactions (e.g., characterize surface albedo, roughness, and evapotranspiration [16]).

While the geometric-optical models have been tested in woodland and savanna using Landsat Multispectral Scanner (MSS), Thematic Mapper (TM), and TM Simulator data [7], [10], [17]-[19], and similar approaches have been applied in woodlands using MSS and aircraft data [20]-[22], they have never been applied to shrub vegetation. Related spectral mixture models have been tested in desert shrub and grassland [23] including some that incorporate geometric modeling of plant shadows [24], but in those studies only plant cover was estimated (not size and density).

Further, the Li–Strahler model has not previously been inverted using SPOT imagery. SPOT HRV XS data have greater spatial resolution (20 m x 20 m pixels) but fewer spectral bands (three) than TM. Given the spatial resolution, the assumption that the pixel is much larger than the average plant canopy, but small enough that the number and size of plants varies among pixels, is likely to be true for shrub canopies. Fewer spectral bands may decrease the spectral separability of the components in the model. However, because SPOT is a pointable sensor, there is a three-fold greater chance of acquiring a near-nadir image of a study area in a specific time period than from Landsat. SPOT may be used increasingly for regional studies. Therefore, part of the objective of this study was to examine the effect of SPOT XS spatial resolution and spectral "dimensionality" on the estimation of vegetation parameters from the model.

Manuscript received June 1, 1991; revised October 1, 1991. This work was supported by NSF Grant SES-890 841 and NASA Grant NAGW-2031.

J. Franklin is with the Department of Geography, San Diego State University, San Diego, CA 92182.

D. L. Turner is with Ogden Environmental, San Diego, CA 92182.

IEEE Log Number 9105694.

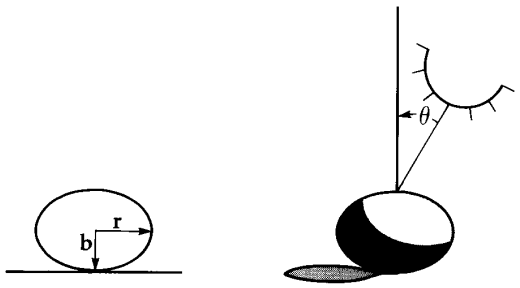

Fig. 1. Shrub shape and illumination geometry for a spheroid.

II. The Canopy Reflectance Model

The Li–Strahler model has been described elsewhere [7], [11], [17] and will be reviewed briefly. A vegetation stand consists of opaque objects (trees or shrubs) that cast shadows onto a spectrally contrasting background (e.g., soil, herbaceous understory, snow). A stand will be defined as an area of vegetation that is relatively homogeneous with respect to composition and structure (average cover or density of plants), i.e., falling within one vegetation class [25]. Pixel reflectance is modeled as the area-weighted sum of the reflectances of four components: illuminated crown, illuminated background, shaded crown, and shaded background. The size and density of plant crowns determine the areal proportions of these components within a pixel. Pixel-to-pixel variance in reflectance occurs because the number of plants and their size varies. Knowledge of the plant shape and illumination geometry can be used to separate canopy from shadow cover, and the variance in pixel reflectance can be used to decompose canopy cover into average plant size and density for the stand. This depends on the following assumptions:

1) A plant can be described as having a simple geometric form that is invariant with size. In this study, shrubs were modeled as spheroids and their shape characterized by the ratio of the vertical (b) to horizontal (r) radius (Fig. 1).
2) The spatial pattern of plants is either random at the scale of sensor resolution, i.e., density counts in pixels can be characterized as a Poisson distribution and C_d, the coefficient of determination (ratio of variance to mean) of counts of plants in pixels set to 1, or if pattern is not random C_d can be estimated from field data.
3) The plant size distribution, expressed as the coefficient of variation (ratio of standard deviation to mean) of squared crown radius, C_{R^2}, has been estimated for the study area, or follows some known distribution function.
4) Plant canopies and background are assumed to be Lambertian reflectors. The four components have distinct multispectral reflectance characteristics or "signatures" (or the canopy and shaded components have a composite signature which is distinct from that of the background), and the signatures are known or can be estimated.

The reflectance (s) of pixel i in band j is:

$$s_{ij} = (A_{g,i}G_j) + (A_{c,i}C_j) + (A_{z,i}Z_j) + (A_{t,i}T_j) \quad (1)$$

where G_j, C_j, Z_j, and T_j are the signatures for an area of sunlit background and crown, and shaded background and crown, respectively, and A_g, A_c, A_z, and A_t are equal to the areal proportion (projected cover) of each component within the pixel. (The subscripts i, j will be dropped for convenience).

By defining X_0 as the average signature of a plant and its associated shadow (a weighted average of C, T, and Z), (1) can be simplified to a two-component mixture model:

$$s = A_gG + (1 - A_g)X_0 \quad (2)$$

In this study as in previous ones, [7], [18], the two-component model was used. Field reflectance measurements indicated that this was reasonable for the study area, at least in the absorptive (green and red) SPOT wavebands (Fig. 2(a) and [26]). The variables describing the stand are:

A	Area of a pixel.
n	Number of plants in a pixel.
N	Average density per unit area of plants in a stand.
${R_p}^2$	Average squared crown radius per pixel (proportional to crown area).
${R_s}^2$	Average ${R_p}^2$ for all pixels in a stand.
m	Product of the density and the average squared crown radius divided by the pixel area ($n{R_p}^2/A$); proportional to the nonoverlapping plant cover in the pixel, $m\pi$.
M	Mean of m for all pixels in the stand; can be approximated by $N{R_s}^2$ divided by the stand area.

A geometric factor Γ, a function of plant shape (the ratio of r to b) and solar zenith angle, is used to adjust crown area to include shadow, such that the area of a pixel covered by a plant and its shadow is $m\Gamma$ (equal to $A_c + A_t + A_z$). The amount of nonoverlapping plant cover in a pixel can be determined by rearranging (1):

$$m = \frac{G - s}{\Gamma(G - X_0)}. \quad (3)$$

Once m is found for each pixel in the stand, the variance of m can be determined. We used the following approximations:

$$M = \frac{G - S}{\Gamma(G - X_0)}. \quad (4)$$

and

$$V(m) = \frac{V(S)}{\Gamma(G - X_0)^2} \quad (5)$$

where S is the average and $V(S)$ is the variance of pixel reflectance for the stand.

The model can be inverted to predict plant size (modified from [7]):

$$R_s^2 = \frac{[(C_d + {C_{R^2}}^2)^2M^2 + 4V(m){C_d}{C_{R^2}}^2]^{1/2} - (C_d + {C_{R^2}}^2)M}{2{C_d}{C_{R^2}}^2}. \quad (6)$$

Franklin and Strahler [18] used the approximation:

$${R_s}^2 = \frac{V(m)}{(C_d + {C_{R^2}}^2)M}. \quad (7)$$

Once ${R_s}^2$ is known, N is easily determined.

TABLE I
SHRUB CLASSES: SHAPE PARAMETERS BASED ON n_1 FIELD MEASUREMENTS; r, HORIZONTAL CROWN RADIUS; b, VERTICAL CROWN RADIUS; Γ FOR THE IMAGE DATES; THE COEFFICIENT OF DETERMINATION OF DENSITY, C_d, BASED ON PHOTOINTERPRETED COUNTS IN 25 PIXELS; THE AVERAGE ($R_s{}^2$) AND THE COEFFICIENT OF VARIATION (C_{R^2}) OF SQUARED CROWN RADIUS, BASED ON PHOTOINTERPRETED CROWN RADIUS OF n_2 SHRUBS

Class								Γ	
Shrub Type	LTER Site	Biomass Class	n_1	$r(m)$	(sd)	$b(m)$	(sd)	June	Sept.
Tarbush	East	low	43	0.46	(0.17)	.35	(.09)	3.7	4.4
Tarbush	Taylor	high	38	0.38	(0.13)	.37	(.08)	3.9	4.9
Creosote	Sand	high	50	0.78	(0.29)	.59	(.19)	3.7	4.5
Mesquite	West	low	49	0.63	(0.57)	.33	(.24)	3.5	4.0
Mesquite	Rabbit	high	52	1.80	(1.25)	.57	(.26)	3.4	3.6

Class		Average	Range	Range	Photointerpreted		
		C_d	C_d	C_{R^2}	$R_s{}^2(m)$	(sd)	n_2
Tarbush	East	2.56	0.76–6.59	0.90–1.27	0.195	(0.209)	2417
Tarbush	Taylor	4.77	1.25–5.63	0.99–1.45	0.239	(0.283)	1884
Creosote	Sand	4.91	1.46–5.63	0.95–1.30	0.307	(0.345)	2045
Mesquite	West	2.95	1.00–5.90	1.46–2.40	0.558	(1.144)	1411
Mesquite	Rabbit	1.03	0.61–1.35	0.91–1.30	2.725	(3.939)	263

Application of the model to shrub canopies will affect the geometric form and the stand variance ($V(S)$). Shrub canopies generally have a larger ratio of canopy diameter to total height than trees and cast less shadow per unit crown area. This could reduce the contrast between X_0 and G, especially in the near-infrared (Fig. 2(a)), degrading the sensitivity of the model. Alternatively, because X_0 will be similar to C, and Γ to π, the model will be less affected by variations in those parameters. Secondly, the average canopy in this study is 40–800 times smaller than the pixel (Table I), while the densities (10–100 plants per pixel) are similar to those found in previous studies of trees where the pixel/canopy area ratio ranged from 20–200 [17]. Therefore, in the present study cover in each pixel is likely be close to the stand mean [14], lowering interpixel variance and reducing the sensitivity of the model.

III. THE STUDY AREA

The Jornada del Muerto basin in southwestern New Mexico, home to the National Science Foundation's Jornada Long Term Ecological Research (LTER) site, has undergone dramatic and well documented vegetation changes in the past century [27] as have large areas of southern New Mexico [28] [29]. Perennial grasslands have been replaced by shrublands over a large extent in the basin, with associated soil erosion and geomorphic changes. Current ecological research in the Jornada LTER is aimed at simulation modeling of the processes leading to this vegetation transition [30], namely changes in the spatial and temporal distribution of water and nutrients between landform elements as a result of the loss of herbaceous cover [31], [32]. Remote sensing research in the Jornada basin has been aimed at estimating the vegetation and soil parameters that are indicators of this form of land degradation [33], [34].

The LTER study area (32°19′N, 106°42′W) is located in the south end of the basin, approximately 37 km north of Las Cruces, NM, on the New Mexico State University College Ranch and USDA Jornada Experimental Range. The study area is described in [31] and [32]. Inter- and intra-annual patterns of primary production are currently being monitored by the LTER investigators on large (70 x 70 m) plots in 15 vegetation classes: three biomass classes (high, medium, and low) in each of five community types, including three shrub and two grassland types (L. Huenneke, pers. comm.) (Fig. 3). The three shrub types are tarbush (dominated by *Flourensia cernua*), creosote bush (dominated by *Larrea tridentata*), and mesquite (dominated by *Prosopis glandulosa*). In the present study, the canopy model was tested in five of the nine shrub-dominated classes (Table I).

IV. METHODS AND DATA SOURCES

A. Parameters Measured in the Field

In order to characterize shrub shape, height and crown diameter were measured for 40–50 plants within circular plots adjacent to the LTER biomass plots (one plot per class, Table I). The geometric parameter Γ (Table I) was calculated using the average ratio of r to b and the solar zenith angle at the time of the acquisition of each SPOT scene (Fig. 1).

B. Aerial Photography

True color aerial photographs of the Jornada study area were acquired on Sept. 29, 1989 at a nominal scale of 1:2500. The photographs were used to: 1) locate the sample stands used to test the model, and for each stand; 2) enumerate shrub density (n); 3) sample crown size (estimate $R_s{}^2$ and C_{R^2});

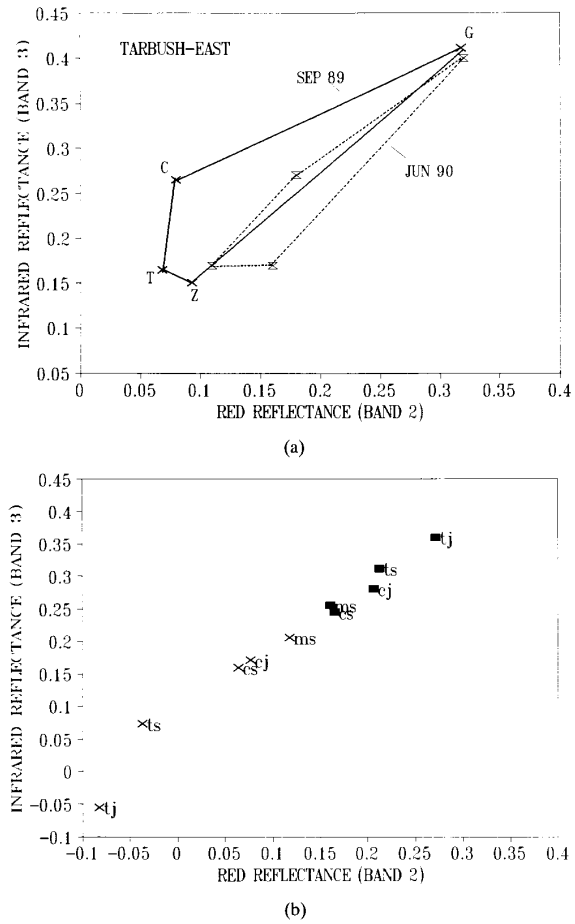

Fig. 2. Red versus infrared reflectance of (a) the four component signatures sampled using an Exotech radiometer and SPOT bandpass filters near the Tarbush-East LTER site in September 1989 and June 1990. Means of 10–20 observations are plotted, G - sunlit soil, Z - shaded soil, C - sunlit shrub, T - shaded shrub; (b) the two components predicted from the model, averaged by type; (X) X_0, (square) G; t - tarbush, c - creosote bush, m - mesquite, j - June image, s - September image.

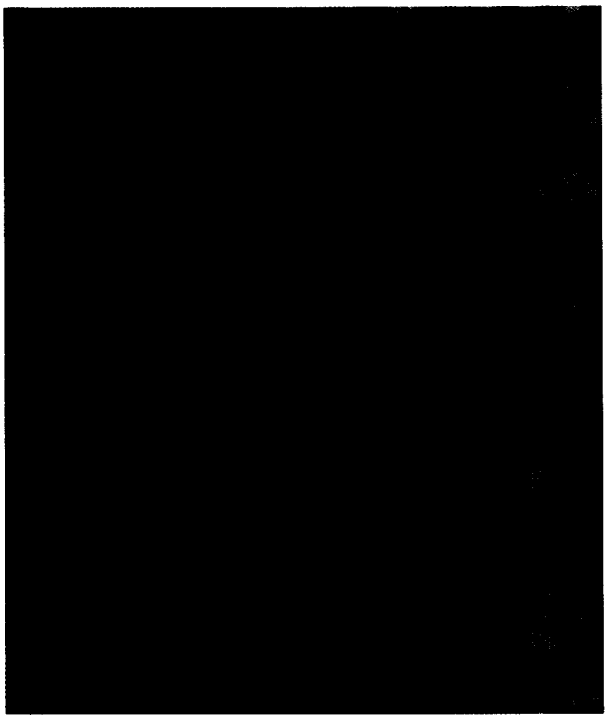

Fig. 3. False-color composite of September 1989 SPOT XS subimage (approximately 15 x 10 km) of the study area showing the extent of the air photo coverage (polygons outlined), the LTER biomass plots (L), the 26 stands used in the study (small boxes), and other landmarks.

and 4) establish the spatial pattern of plants (determine C_d). The model was tested in 26 one-ha stands (equal to 5 x 5 SPOT pixels), 5–6 in each shrub stratum. Sample stands were selected if they were:

- within the limited air photo coverage (flight lines only included the 15 LTER biomass plots),
- at least 100 m apart if possible (to avoid autocorrelation among the vegetation parameters),
- at least 25 m from a road,
- near the LTER sites and appearing to fall within the same vegetation classes as them.

The stands were chosen subjectively, from 74 stands used in [35], to span a range of shrub cover values. Given the photo coverage, the choice of 1-ha nonoverlapping stands was limited, and some sites were close together (Fig. 3).

Shrub size and density measurements were required to assess the accuracy of the model. Density was determined for each of the stands by mapping the point locations of all shrubs from the air photos using a Zoom Transfer Scope. The spatial pattern of shrubs was described by the coefficient of dispersion of density (C_d), calculated from the counts of shrubs in pixel-sized contiguous quadrats (called pixels for simplicity) for each stand [7], [36]. Crown size was determined by measuring the diameters of shrubs in the photos (magnified to a nominal scale of 1:200) in a subsample of five randomly chosen pixels or 20% of the stand. C_{R^2} was calculated based on the 250–2500 crowns measured in each stand using the photos (Table I).

C. Satellite Imagery

SPOT images of the study area were acquired on June 12 and Sept. 24, 1989, and used to test the model. The SPOT XS sensor records radiance in the green (.50–.59 μm), red (.61–.68 μm) and near-infrared (.79–.89 μm) wavebands. The images were nominally corrected for variations due to atmospheric effects and changes in solar elevation using a dark-object subtraction method, and the reflectance was calculated for each pixel using the method described in [37], so that the digital number in the transformed image corresponds to reflectance multiplied by 255. The images were also geometrically referenced to a UTM projection based on ground control points and nearest neighbor resampling. The stands were located in the images visually using the many roads, arroyos and other features prominent in both the imagery and the air photos (Fig.

TABLE II
REGRESSION SLOPES (A), INTERCEPTS (B) AND r^2 FOR THE BACKGROUND (G) AND SHRUB/SHADOW (X_0) SIGNATURES, USED TO ESTIMATE SIGNATURES FROM THE MAXIMUM AND MINIMUM REFLECTANCE NUMBERS IN EACH STAND USING IMAGERY FROM EACH DATE

		G			X_0		
Type	Band	A	B	r^2	A	B	r^2
September							
Tarbush	all	1.40	4.65	0.97	0.98	-41.22	0.54
Creosote	all	1.00	2.71	0.99	1.06	-18.92	0.56
Mesquite	all	1.00	0.31	0.99	0.92	-2.69	0.94
June							
Tarbush	1				1.23	-54.14	0.04
	2	1.13	-0.27	0.98	2.76	-150.79	0.19
	3				2.25	-161.58	0.12
Creosote	all	1.01	2.21	0.99	0.99	-21.19	0.56

3). Reflectance statistics (minimum, maximum, S and $V(S)$ in each band) were extracted for the stands, and were used to determine signatures for G and X_0, and to invert the model.

D. Testing the Model

Component signatures G and X_0 were first modeled in each spectral band utilizing the satellite image data and known values of N, ${R_s}^2$, C_{R^2}, C_d and for each stand. Equations (4)-(6) were used to predict the signatures by solving for G and X_0. These modeled values of G and X_0 were related to the minimum and maximum reflectance numbers for each stand using linear regression, and then the regression coefficients were used to estimate component signatures in each site from the minimum and maximum reflectance in each band [18]. The estimated component signatures (G_E, X_{oE}) were then used with the stand parameters (Γ, C_{R^2}, C_d), and the reflectance statistics ($S, V(S)$) for each spectral band, to estimate the size and density (${R_s}^2$ and N) of shrubs in a stand from both (6) and (7). Thus there were three predictions (from the three SPOT bands) of size and density per stand for each equation, and instead of averaging this small number of predictions, the median value was chosen [18]. Note that testing the model on the same stands used to estimate the signatures will tend to overestimate model performance.

E. Assessing Model Performance

Predicted and observed shrub size and density were compared using the following statistics: the mean absolute percent error (MAPE),

$$\text{MAPE} = \frac{1}{K}\sum_{k=1}^{K}\frac{|P_k - O_k|}{O_k} \tag{8}$$

the mean absolute error (MAE),

$$\text{MAE} = \frac{1}{K}\sum_{k=1}^{K}|P_k - O_k| \tag{9}$$

and the mean percent error (MPE),

$$\text{MPE} = \frac{1}{K}\sum_{k=1}^{K}\frac{P_k - O_k}{O_k} \tag{10}$$

where K is the number of stands, P_k is the predicted, and O_k is the observed size or density for stand k [38]. The MAPE expresses error as a proportion of the observed values, the MAE is in the units of the variable being predicted, and the MPE can reveal systematic errors in the predictions.

The accuracy based on all stands was evaluated for several trials designed to examine the effect of the time of year of the image acquisition (related to plant phenology and canopy shadowing), and the parameter describing shrub spatial pattern (C_d), on the model performance. Three trials were run using the September (end of the summer growing season) image data: a) C_d was set to one [9], b) C_d was set to the actual value calculated for each stand (Table I), and c) C_d was set to an average value for the shrub type (a value of 3 was used for all but the Mesquite-Rabbit class where C_d was set to 1). Then for the June (early in the summer growing season) image, the model was tested using the value of C_d that gave the best results in the previous trials. Finally, the accuracy for each shrub class was evaluated based on the best trial, using the same statistics.

V. RESULTS

A. Estimation of Signatures

Signatures were modeled and estimated separately for each shrub type and for each trial (because C_d enters into the calculation). For most trials, there was a linear relationship between the modeled signatures and extreme reflectance values for the stands for all bands combined. The relationship was much stronger for G than for X_0 (Table II). However, the model is more sensitive to the accurate characterization of G [18].

In general, for both signatures, the slope was close to one, except for the tarbush type in the June imagery. The intercept was small and positive for G, so that the estimated background signature was always slightly brighter than the brightest pixel in the stand. If there are no pixels of pure background (or vegetation) in the stand, the model will predict a signature for G (or X_0) that is brighter (darker) than the maximum (minimum) reflectance. The intercept was large and negative for X_0, so that estimated X_0 was always much darker than the darkest pixel in the stand, resulting in a negative value in some cases. Negative values would not be expected for calibrated satellite data, and could indicate either that satellite data were not perfectly calibrated, or that $V(S)$ contains noise variance (from variance in G or X_0), causing X_0 to be underestimated.

TABLE III
OVERALL MODEL RESULTS SHOWING THE MEAN ABSOLUTE ERROR (MAE), MEAN ABSOLUTE PERCENT ERROR (MAPE), AND MEAN PERCENT ERROR (MPE) OF CROWN AREA (m^2) AND DENSITY (PER ha) FOR THE DIFFERENT TRIALS

Trial	MAE	MAPE	MPE
CROWN AREA (m^2)			
September Image (26 sites)			
Observed C_d	1.24	0.41	0.01
$C_d = 1$	1.20	0.40	0.02
Average C_d by stratum	1.16	0.35	-0.07
June Image (16 sites)			
Average C_d by stratum	0.32	0.40	0.07
DENSITY (per ha)			
September Image (26 sites)			
Observed C_d	702	0.43	0.19
$C_d = 1$	525	0.38	0.20
Average C_d by stratum	452	0.31	0.17
June Image (16 sites)			
Average C_d by stratum	275	0.15	0.01

All bands could be grouped for signature estimation because the desert soils in these sites are brighter than shrub canopy in all wavebands (including band 3, the near-infrared). The only time this was not the case (and X_0 signatures had to be estimated separately for each band) was again for the tarbush type in the June imagery (Table II).

B. Accuracy of Model Predictions

Results from (6) and (7) were nearly identical and all results presented below are based on (7). The overall accuracy was highest for the trials run using the September imagery when an average value of C_d for each stratum was used, lowest when the observed value of C_d for each stand was used, and intermediate when C_d was set equal to one (Table III). The MPE shows that density was systematically overestimated and size underestimated in the September trials where an average C_d was used (Fig. 4). The MAPE (30–43%) indicates that overall accuracy of the model is low for both dates.

It was expected that the June image data would yield more accurate predictions. In June, at the beginning of the summer growing season, the deciduous tarbush and mesquite have started to leaf out, and the evergreen creosote bush is growing new leaves, but the perennial and annual grasses have not yet greened up [39]. Therefore, the contrast between the shrub layer and background should be greatest at that time. In September, grass cover, extensive in some areas (especially in the tarbush type) may cause both reduced contrast between G and X_0 and increased variance in G among pixels, which reduce the accuracy of the model [18]. However, the June 1989 image of the Jornada contained both nonsystematic noise in some portions of the image (preventing the mesquite stands from being examined), and systematically higher reflectance numbers than the September image in all bands, even after atmospheric correction [35]. A systematic offset should not affect the results of the canopy model; however, unobserved nonsystematic noise could degrade the results. The MAE's of the June results can not be compared directly to September results because they are based on a smaller number of stands,

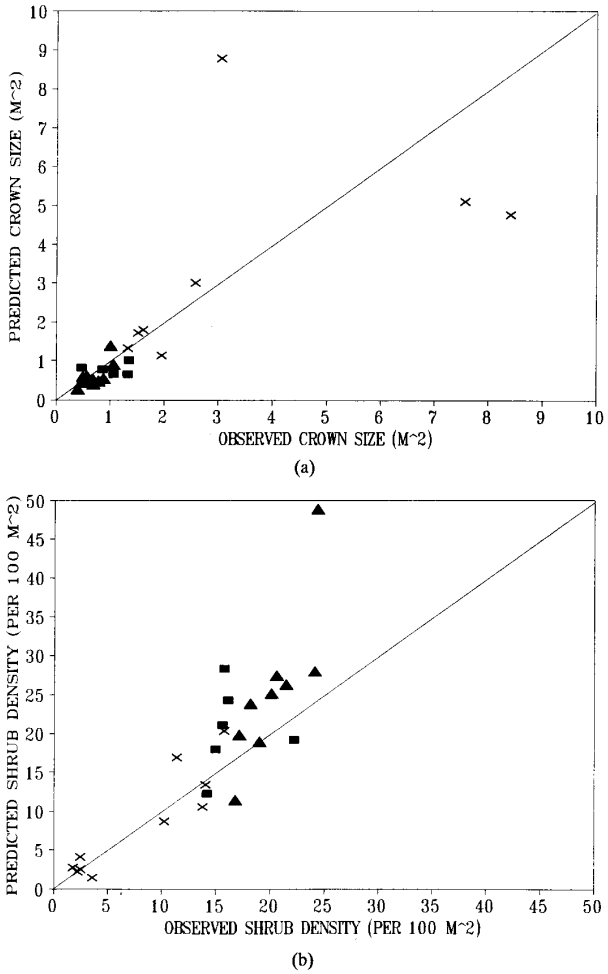

Fig. 4. Observed versus predicted (a) shrub size (crown area in m^2), and (b) density (shrubs per 100 m^2) for the (triangle) tarbush, (square) creosote bush, and (X) mesquite stands. Diagonal is the 1:1 line.

but the MAPE for crown size was roughly the same while MPE indicates that size was overestimated. MAPE for density was lower and the predictions were unbiased (Table III).

When the stands are grouped by shrub class the results based on both image dates are more encouraging. Table IV shows the average observed and predicted values for the 5–6 stands within each class, and the accuracy statistics, based on the average C_d trial. The MAPE varied greatly among strata, and values ranged around the overall figures (15–40%) with the exception of crown size for Mesquite-Rabbit (67%). However, predicted values were often within the range of observed values for the stratum, i.e., the MAE's were usually within one standard deviation of the observed values for size, even for Mesquite-Rabbit, and within two standard deviations of the observed values for density (but the sample size for each class was small). Also, the rank order of the predicted and observed average size and density were the same. In other words, the model is differentiating among the canopy structures represented by these five classes. The means and

TABLE IV
MODEL RESULTS SHOWING THE OBSERVED AND PREDICTED AVERAGE VALUES OF CROWN SIZE AND DENSITY FOR EACH CLASS, THEIR STANDARD ERRORS, AND THE THREE ACCURACY STATISTICS

Class		n	Obs.	(*sd*)	Pred.	(*sd*)	MAE	MAPE	MPE
SEPTEMBER									
Crown Area (m^2)									
Tarbush	East	5	0.62	(0.15)	0.45	(0.41)	0.20	0.32	-0.25
Tarbush	Taylor	5	0.80	(0.27)	0.78	(0.34)	0.19	0.21	-0.02
Creosote	Sand	6	1.02	(0.33)	0.79	(0.12)	0.37	0.38	-0.14
Mesquite	West	5	1.79	(0.49)	1.80	(0.65)	0.33	0.17	0.00
Mesquite	Rabbit	5	9.72	(6.02)	7.14	(1.82)	4.87	0.67	0.08
Density (per ha)									
Tarbush	East	5	2286	(319)	3019	(944)	912	0.39	0.33
Tarbush	Taylor	5	1902	(299)	2042	(551)	351	0.19	0.06
Creosote	Sand	6	1644	(290)	2099	(535)	569	0.35	0.26
Mesquite	West	5	1303	(222)	1333	(467)	347	0.28	0.01
Mesquite	Rabbit	5	294	(66)	259	(87)	96	0.36	0.12
JUNE									
Crown Area (m^2)									
Tarbush	East	5	0.62	(0.15)	0.46	(0.18)	0.15	0.26	-0.26
Tarbush	Taylor	5	0.80	(0.27)	0.93	(0.31)	0.24	0.32	0.20
Creosote	Sand	6	1.02	(0.33)	0.90	(0.13)	0.32	0.40	0.07
Density (per ha)									
Tarbush	East	5	2286	(319)	3123	(1267)	1067	0.45	0.33
Tarbush	Taylor	5	1902	(299)	1818	(599)	405	0.22	-0.06
Creosote	Sand	6	1644	(290)	1655	(174)	275	0.15	0.01

standard deviations reported for crown size in Table IV are grand means of the means for each stand within a class. The variances of all photointerpreted crown size measurements for individual shrubs within a class were much higher (Table I). Overall, there does not seem to be a consistent improvement in the results by class based on the June imagery.

VI. DISCUSSION AND CONCLUSION

The large errors in model predictions are a result of a) poor estimation of component signatures, b) a weak relationship between $V(S)$ and shrub size, and c) low $V(S)$, leading to low model sensitivity. Errors would presumably be even larger if the model were tested on an independent set of stands. The signature estimation procedure yielded realistic values for the background signature, G, considering that field-sampled G shown in Fig. 2(a) was based on soil only and did not include litter or herbaceous vegetation. However, unrealistic X_0 signatures were predicted (Fig. 2(b)), and they were poorly related to stand reflectance characteristics as indicated by the low r^2 values in Table II. A possible solution would be to estimate the X_0 signature from field data, holding it constant for a vegetation type, and only estimate G from the stand histogram. Alternatively, G could be a variable, predicted from the model, if some other parameter were known, such as the distribution of *b/r* (X. Li, pers. comm.).

Further, large errors resulted because the stand spectral variance, $V(S)$, was not closely related to shrub size. Even within a vegetation type there were stands with high $V(S)$ and relatively small shrubs. If the true variance was poorly estimated from the 25 observations in the 1-ha stands, then an image segmentation procedure that delineates stands composed of more pixels might characterize $V(S)$ better [19]. Alternatively, if $V(S)$ is strongly affected by within-stand variance in G, there are two possible solutions: a) band transformations might reduce the variance in G; b) a fixed proportion of $V(S)$ could be attributed to $V(G)$, perhaps as a function of vegetation type, and the remaining variance used to predict crown size.

Finally, if $V(S)$ is low because the shrubs are very small relative to the pixel size, shrub spatial pattern is regular, or because of poor contrast between G and X_0, the problem is poorly posed. For many of the creosote bush and mesquite sites the variance was only 1–2 reflectance numbers (< 1% reflectance) in the three SPOT bands.

The systematic errors in the predictions based on average C_d may have occurred because the value used for most stands (3) overcompensated for the effect of a clumped spatial pattern in some cases. In those tarbush-east and creosote stands where C_d was actually less than 3, crown size was underestimated and density overestimated because too much of the variance in reflectance was attributed to variation in density rather than larger crown size. This pattern of errors could also result if crown size was more variable for sparse stands, and less so for dense stands. However, this was not observed in the estimated values of C_{R^2} (Table I).

In the June imagery, $V(S)$ was not lower than in September as hypothesized, but, in fact, was higher in band 3 and varied by site in bands 1 and 2. It is not known if this is due to radiometric noise in the June satellite data (noted above) or to variations in the phenology of shrubs or other vegetation.

The simple model that was used assumes no overlap of crowns and shadows, a reasonable assumption for low plant

cover (independently estimated crown cover ranged from 20–45% in the stands [35]). However, in the case of a clumped spatial pattern, overlap could occur even at intermediate densities. If overlap is present, application of the nonoverlapping model would result in underestimation of size (and density) in higher-cover stands. While size was underestimated in the tarbush and creosote classes density was overestimated and it is more likely that the error is related to signature estimation and to the parameter C_d as noted above.

The Jornada data set could be used to test more complex versions of the geometric optical canopy model by:

- using the four spectral components, and exploring the trade-off between this and including additional background spectral components, which necessitates using TM or other data with more spectral wavebands;
- predicting m for each pixel based on multiple bands and a maximum likelihood, look-up table approach, using the overlap model [19];
- using larger stands, in order to better estimate component signatures and stand spectral variance, and more of them, to allow for cross validation of the model results.

The importance of the invertible discrete-object reflectance models is that, while other empirical and deterministic remote sensing models predict a single parameter (biomass, cover, leaf area index) from a reflectance or spectral index value, the invertible models use the average reflectance of a stand and its spatial variance to estimate two parameters of vegetation structure, plant size and density. These parameters are more closely related to primary productivity [40], surface roughness, and other important biophysical parameters [15] of woody vegetation than cover alone.

ACKNOWLEDGMENT

The authors acknowledge the support of the Jornada LTER consortium, with special thanks to J. Anderson, J. Duncan, A. Hope, L. Huenneke, D. Lightfoot, E. Muldavin, J. Reynolds, D. Stow, R. Virginia, and W. Whitford. We are also greatly indebted to D. McKinsey, X. Li, A. Strahler, and the anonymous reviewers.

REFERENCES

[1] N. S. Goel, "Inversion of canopy reflectance models for estimation of biophysical parameters from reflectance data," in *Theory and Application of Optical Remote Sensing*, G. Asrar, Ed. New York: John Wiley and Sons, 1989, pp. 205–251.

[2] A. J. Richardson and C. L. Wiegand, "Distinguishing vegetation from soil background information," *Photogrammetr. Eng.*, vol. 43, pp. 1541–1552, 1977.

[3] R. D. Graetz and M. R. Gentle, "The relationship between reflectance in the Landsat wavebands and the composition of an Australian semiarid shrub rangeland," *Photogrammetric Engineering and Remote Sensing*, vol. 48, pp. 1721–1730, 1982.

[4] A. R. Huete, "A soil-adjusted vegetation index (SAVI)," *Remote Sensing Environment*, vol. 25, pp. 295–309, 1988.

[5] R. D. Graetz, R. P. Pech, M. R. Gentle, and J. F. O'Callaghan, "The application of Landsat image data to rangeland assessment and monitoring: the development and demonstration of a land image based resource information system (LIBRIS)," *J. Arid Environments*, vol. 10, pp. 53–80, 1986.

[6] A. R. Huete and R. D. Jackson, "Suitability of spectral indices for evaluating vegetation characteristics on arid rangelands," *Remote Sensing Environment*, vol. 23, pp. 213–232, 1987.

[7] X. Li and A. H. Strahler, "Geometric-optical modeling of a conifer forest canopy," *IEEE Trans. Geosci. Remote Sensing*, vol. GE-23, pp. 705–721, 1985.

[8] X. Li and A. H. Strahler, "Geometric-optical bidirectional reflectance modeling of a conifer forest canopy," *IEEE Trans. Geosci. Remote Sensing*, vol. GE-24, pp. 906–919, 1986.

[9] X. Li and A. H. Strahler, "Modeling the gap probability of a discontinuous vegetation canopy," *IEEE Trans. Geosci. Remote Sensing*, vol. GE-25, pp. 161–170, 1988.

[10] D. L. B. Jupp, J. Walker, and L. K. Penridge, "Interpretation of vegetation structure in Landsat MSS imagery: a case study in disturbed semiarid eucalypt woodlands. Part 2. Model-based analysis," *J. Environmental Management*, vol. 23, pp. 35–57, 1986.

[11] A. H. Strahler and D. L. B. Jupp, "Geometrical-optical modeling of forests as scenes composed of three-dimensional discrete objects," in *Photon–Vegetation Interactions: Applications in Optical Remote Sensing and Plant Ecology*, R. B. Myneni and J. Ross, Eds. Heidelberg, Germany: Springer-Verlag, 1991, pp. 153–166.

[12] A. H. Strahler and D. L. B. Jupp, "Modeling bidirectional reflectance of forests and woodlands using boolean models and geometric optics," *Remote Sensing Environment*, vol. 34, pp. 153- 166, 1991.

[13] D. L. B. Jupp, A. H. Strahler, and C. E. Woodcock, "Autocorrelation and regularization in digital images I. Basic theory," *IEEE Trans. Geosci. Remote Sensing*, vol. 26, pp. 463–473, 1988.

[14] D. L. B. Jupp, A. H. Strahler, and C. E. Woodcock, "Autocorrelation and regularization in digital images II. Simple image models," *IEEE Trans. Geosci. Remote Sensing*, vol. 27, pp. 247–258, 1989.

[15] R. D. Graetz, "Remote sensing of terrestrial ecosystem structure: an ecologist's pragmatic view," in *Remote Sensing of Biosphere Functioning*, R. J. Hobbs and H. A. Mooney, Eds. New York: Springer-Verlag, 1990, pp. 5–30.

[16] P. J. Sellers, F. G. Hall, D. E. Strebel, G. Asrar, and R. E. Murphy, "Satellite remote sensing and field experiments," in *Remote Sensing of Biosphere Functioning*, R. J. Hobbs and H. A. Mooney, Eds. New York: Springer-Verlag, 1990, pp. 169–201.

[17] A. H. Strahler, Y. Wu, and J. Franklin, "Remote estimation of tree size and density from satellite imagery by inversion of a geometric-optical canopy model," in *Proceedings of the Twenty-Second International Symposium on Remote Sensing of the Environment*, Abidjan, Cote d'Ivoire, Oct. 20–26, 1988, pp. 337–348.

[18] J. Franklin and A. H. Strahler, "Invertible canopy reflectance model of vegetation structure in semiarid woodland," *IEEE Trans. Geosci. Remote Sensing*, vol. GE-26, pp. 809–825, 1988.

[19] C. E. Woodcock, V. Jokabhazy, S. Ryherd, A. H. Strahler, and Y. Wu, "Timber inventory using Landsat Thematic Mapper imagery and canopy reflectance models," in *Proceedings of the 23th International Symposium on Remote Sensing of Environment*, vol. 2, pp. 937–948, 1990.

[20] R. P. Pech and A. W. Davis, "Reflectance modeling of semiarid woodlands," *Remote Sensing Environment*, vol. 21, pp. 365–377, 1987.

[21] M. F. Jasinski and P. S. Eagleson, "Estimation of subpixel vegetation cover using red-infrared scattergrams," *IEEE Trans. Geosci. Remote Sensing*, vol. 28, pp. 253–267, 1990.

[22] M. F. Jasinski, "Functional relation among subpixel canopy cover, ground shadow, and illuminated ground at large sampling scales," in *Proceedings SPIE, Series 3, Remote Sensing of the Biosphere*, Orlando, FL, 19–20 Apr. 1990, vol. 1300, pp. 19–20.

[23] M. O. Smith, S. L. Ustin, J. B. Adams, and A. R. Gillespie, "Vegetation in deserts: A regional measure of abundance from multispectral images," *Remote Sensing Environment*, vol. 31, pp. 1–26, 1990.

[24] R. P. Pech, A. W. Davis, and R. D. Graetz, "Reflectance modeling and the derivation of vegetation indices for an Australian semiarid shrubland," *Int. J. Remote Sensing*, vol. 7, pp. 389–403, 1986.

[25] A. H. Strahler, "Stratification of natural vegetation for forest and rangeland inventory using Landsat digital imagery and collateral data," *Int. J. Remote Sensing*, vol. 2, pp. 15–41, 1981.

[26] D. L. Turner, "Invertible canopy reflectance modeling of semiarid shrub vegetation," Masters thesis, San Diego State University, San Diego, CA, 1991.

[27] L. C. Buffington and C. H. Herbel, "Vegetational changes on a semidesert grassland range from 1858 to 1963," *Ecological Monographs*, vol. 35, pp. 139–164, 1965.

[28] J. C. York and W. A. Dick-Peddie, "Vegetational changes in southern New Mexico during the past hundred years," in *Arid Lands in Perspective*, W. G. McGinnies and B. J. Goldman, Eds. Tucson, AZ: The University of Arizona Press, 1969, pp. 157–166.

[29] H. D. Grover and H. B. Musick, "Shrubland encroachment in southern New Mexico, U.S.A.: an analysis of desertification processes in the American Southwest," *Climatic Change*, vol. 17, pp. 305–330, 1990.

[30] J. F. Reynolds, J. M. Cornelius, D. M. Moorhead, P. R. Kemp, D. W. Hilbert, R. A. Virginia, W. M. Jarrell, W. H. Schlesinger, L. F. Huenneke, and W. G. Whitford, "The response of an arid ecosystem to spatial and temporal variability in resources: a systems modeling approach," manuscript in preparation.
[31] S. M. Wondzell, G. L. Cunningham, and D. Bachelet, "A hierarchical classification of landforms: Some implications for understanding local and regional vegetation dynamics," in *Proceedings Symposium on Strategies for Classification and Management of Natural Vegetation for Food Production in Arid Zones*, Tucson, AZ, Oct. 12–16, 1987, pp. 15–23.
[32] W. H. Schlesinger, J. F. Reynolds, G. L. Cunningham, L. F. Huenneke, W. M. Jarrell, R. A. Virginia, and W. G. Whitford, "Biological feedbacks in global desertification," *Science*, vol. 247, pp. 1043–1048, 1990.
[33] H. B. Musick, "Assessment of Landsat multispectral scanner spectral indices for monitoring arid rangelands," *IEEE Trans. Geosci. Remote Sensing*, vol. GE-22, pp. 512- 519, 1984.
[34] P. L. Warren and C. F. Hutchinson "Indicators of rangeland change and their potential for remote sensing," *J. Arid Environments*, vol. 7, pp. 107–126, 1984.
[35] J. Duncan, "Assessing the relationship between spectral vegetation indices and shrub cover in a semiarid environment," Masters thesis, San Diego State University, San Diego, CA, 1991.
[36] J. Franklin, J. Michaelsen, and A. H. Strahler, "Spatial analysis of density dependent pattern in coniferous forest stands," *Vegetatio*, vol. 64, pp. 29–36, 1985.
[37] P. S. Chavez, Jr., "An improved dark-object subtraction technique for atmospheric scattering correction of multispectral data," *Remote Sensing Environment*, vol. 24, pp. 459–479, 1988.
[38] R. S. Pindyck and D. L. Rubenfeld, *Econometric Models and Econometric Forecasts* (2nd ed.). New York: McGraw Hill, 1981, pp. 360–381.
[39] P. R. Kemp, "Phenological patterns of Chihuahuan desert plants in relation to the timing of water availability," *J. Ecology*, vol. 71. pp. 427–436, 1983.
[40] J. A. Ludwig, J. F. Reynolds, and P. D. Whitson, "Size biomass relationships of several Chihuahuan desert shrubs," *American Midland Naturalist*, vol. 94, pp. 451–461, 1975.

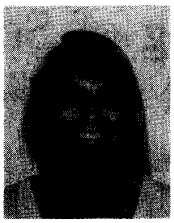

Janet Franklin received the B.A. degree in biology in 1979 and the M.A. and Ph.D. degrees in geography in 1983 and 1988, all from the University of California at Santa Barbara.

She is an assistant professor of geography at San Diego State University, where she is also codirector of the Center for Earth Systems Analysis Research, and a member of the Systems Ecology Research Group. Her primary research focus is canopy reflectance modeling. She is also interested in the remote sensing of natural vegetation for global change research, especially the development of remote sensing algorithms and geographical modeling methods for studying land degradation in semiarid wodland, savanna, and scrub in Africa and the western U.S. Her other research interests include vegetation analysis and spatial landscape analysis to identify critical habitats for the conservation of biodiversity in California and Polynesia.

Debra L. Turner received the B.A. degree in environmental studies from the University of California at Santa Barbara in 1987, and the M.A. degree in geography from San Diego State University in 1991.

She is currently an environmental scientist with Ogden Environmental in San Diego. Her professional interests include plant canopy reflectance modeling, regional ecological modeling, multispecies conservation strategies, restoration of disturbed ecosystems, and the use of remote sensing and geographical information systems for environmental monitoring and modeling.